

Wall-Following Controllers for Sonar-Based Mobile Robots

Alberto Bemporad, Mauro Di Marco, Alberto Tesi

Dipartimento di Sistemi e Informatica
Università di Firenze
Via di S. Marta 3, 50139 Firenze, Italy
Tel. +39-55-479263, Fax +39-55-4796363
atesi@ingfi1.ing.unifi.it

Abstract

For mobile robots equipped with incremental encoders and one sonar sensor this paper presents wall-following controllers that achieve global convergence, as well as the fulfillment of constraints on the orientation of the sonar and the velocities of the wheels. A sensor-fusion approach for the estimation of the robot's coordinates is adopted by designing an Extended Kalman Filter that combines ultrasonic and odometric data.

keywords: Mobile robots, wall-following, extended Kalman filter, Lyapunov functions.

1 Introduction

To move around in the darkness by touching walls and objects with our hands to understand where we are, or learn how places where we have never been before look like, is a natural behaviour. This skill, namely the ability to follow object contours, is also required in many applications of autonomous mobile robots, where “hands” are typically ultrasonic, laser, or infrared sensors, and “darkness” is the absence of more sophisticated sensors, e.g. absolute positioning systems and artificial vision devices.

For indoor environments, this ability is required for three main tasks:

- *Map building:* In unknown environments, as the presence of a new wall is detected, some exploration algorithms command a wall-following in order to collect data on orientation, position, and length of the wall [1, 2, 3].
- *Obstacle avoidance:* The execution of a planned path can be prevented by an unexpected obstacle. When the path cannot be replanned, a simple strategy consists in following the contour of the obstacle by using distance sensors [4].

- *Improvement of the position estimate:* Position and orientation estimates obtained by dead-reckoning methods deteriorate as the length of the travel distance increases, mostly due to unequal wheel diameters and uncertainty about the effective wheelbase [5]. By planning the motion of the robot along straight walls, the error can be reduced by merging odometry with measurements of distance [3, 6], thus arriving at a more suitable strategy for map building applications. This idea is useful also in unknown environments, where the only straightness of the walls can be exploited to reduce odometric errors [7].

In all three the situations, a *sensor fusion* which integrates data from sensors of distance (e.g. sonars) and velocity (typically incremental encoders) is necessary [1, 8, 9, 10]. However, in order to accomplish this, certain operating conditions must be taken into account in designing a wall following controller. Ultrasonic sensors, for instance, require that the difference between the orientation of the surface of the receiver and the wall is sufficiently small, typically no more than $10^\circ - 15^\circ$ [11, 12, 13, 14, 15, 16]. Furthermore, saturation nonlinearities of the motors put a constraint on the velocity of the wheels, thus leading to a discrepancy between the velocities commanded by the controller and the actual velocities of the robot and, consequently, to a loss of information. Henceforth, the orientation and the velocity constraints must be taken into account in designing a wall following controller, if persistent sensor fusion is desired.

For differential-drive mobile robots equipped with two incremental encoders on the driving wheels and one ultrasonic sensor on a side, as the one depicted in Fig. 1, this paper presents a pair controller/observer for wall following. By using a Lyapunov argument, both convergence and constraint fulfillment for all the starting conditions which satisfy these constraints is proved.

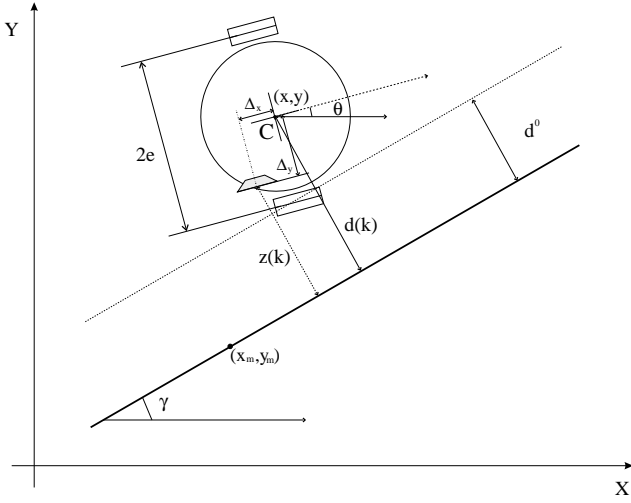


Figure 1: Wall Following Problem (WFP).

The control scheme is equipped with an on-line time-scaling algorithm to enforce constraints on the velocity commands generated by the controller, without deteriorating the convergence properties. Sensor fusion happens mostly at the observer level: an Extended Kalman Filter (EKF) updates positions and orientation estimates by merging velocity and distance measures, thus making this designed controller suitable for map building applications.

The paper is organized as follows. In Section 2 we formulate the wall following problem. Section 3 is devoted to present a wall-following controller+observer which guarantees constraints fulfillment and possesses global asymptotical properties. Some experimental results are finally reported in Section 4.

2 Problem Formulation

Consider a differential-drive mobile robot whose coordinates (x, y, θ) are related by the kinematic equations

$$\begin{cases} \dot{x} &= v \cos \theta \\ \dot{y} &= v \sin \theta \\ \dot{\theta} &= \omega \end{cases} \quad (1)$$

where x and y denote the position in the Cartesian space, θ the orientation (angle between the x -axis and the axis of the robot), v and ω the linear and the angular velocity of the robot, respectively. These depend on the angular velocities ω_1, ω_2 through the relation

$$\begin{cases} r\omega_1 &= v + e\omega \\ r\omega_2 &= v - e\omega \end{cases} \quad (2)$$

where r is the wheel radius, and e half the wheelbase (distance between wheel contact points). We wish to solve the following problem (see Fig. 1):

(WFP) Wall Following Problem. *For the perfectly straight and infinite wall described in the Cartesian*

plane by the equation

$$(x - x_m) \sin \gamma - (y - y_m) \cos \gamma = 0 \quad (3)$$

determine a feedback control law such that the mobile robot (1) moves at a constant speed v_{des} along the wall at a distance d^0 from it.

In (3) (x_m, y_m) and γ are respectively a representative point and the orientation of the wall, expressed in the same Cartesian space chosen to describe the robot's position.

2.1 Ideal Wall-Following Problem (IWFP)

Assume that the coordinates (x, y, θ) are perfectly measurable and the robot dynamics is negligible, in that command inputs can be given at the velocity level. A solution to the wall-following problem in this ideal framework is provided by the control law

$$\begin{cases} v &= v_{des} \\ \omega &= -\frac{k(d - d^0)}{v_{des} \cos(\theta - \gamma)} - \beta \tan(\theta - \gamma) \end{cases} \quad (4)$$

where k and β are positive scalar and d is the distance of the mobile robot from the wall, i.e., $d = (y - y_m) \cos \gamma - (x - x_m) \sin \gamma$. In fact, setting $x_1 \triangleq d - d^0$, $x_2 \triangleq \dot{d}$, the closed loop equation (1)-(4) have the form

$$\begin{cases} \dot{x}_1 &= x_2 \\ \dot{x}_2 &= -kx_1 - \beta x_2 \end{cases} \quad (5)$$

Therefore, for any initial condition, it results $d(t) \rightarrow d^0$, $\dot{d}(t) \rightarrow 0$, and $\sin(\theta(t) - \gamma) \rightarrow 0$ as $t \rightarrow \infty$.

2.2 Real Wall-Following Problem (RWFP)

Consider the practical situation where the robot is equipped with DC motors as velocity command actuators, incremental wheel encoders as velocity sensors, and a single sonar is mounted on the robot, as depicted in Fig. 1. In this situation, the saturation nonlinearities of the DC motors may prevent the use of large velocity commands, while the encoder and sonar measures are inevitably corrupted by the noise. Moreover, the sonar can collect useful data only when the direction orthogonal to the reflecting surface lies within the beamwidth of the receiver, thus allowing for the detection of the wall only for restricted ranges of orientation. These aspects are not taken into account in the control law (4) and the behaviour of the mobile robot may result quite deteriorated.

To arrive at a satisfactory RWFP formulation, the above aspects have to be translated into suitable relations among the system variables. The beamwidth leads to the following orientation constraint

$$|\theta - \gamma| \leq \sigma_{max} \quad (6)$$

where typically $\sigma_{max} \in [10^\circ, 15^\circ]$. If Ω_{max} is the maximum allowable angular velocity of the wheels, i.e.,

$|\omega_1|, |\omega_2| \leq \Omega_{max}$, taking into account (2), the following velocity constraints are obtained

$$|v \pm \epsilon\omega| \leq r\Omega_{max} \quad (7)$$

Due to the measure errors, only an estimate $(\hat{x}, \hat{y}, \hat{\theta})$ of the coordinates (x, y, θ) is available by suitably relating the encoder and sonar measures. Suppose that the measures are collected every T_c seconds and let $\omega(k)$ and $v(k)$ denote the angular and linear velocity measured at time kT_c by the encoders, while $z(k)$ indicate the distance measured at time kT_c by the sonar. Then, an estimate $(\hat{x}, \hat{y}, \hat{\theta})$ can be obtained through the following model consisting of the integration of (1) by Simpson's Rule

$$\begin{cases} x(k) \approx x(k-1) + \frac{T_c}{2} (v(k) \cos \theta(k) + v(k-1) \cos \theta(k-1)) \\ y(k) \approx y(k-1) + \frac{T_c}{2} (v(k) \sin \theta(k) + v(k-1) \sin \theta(k-1)) \\ \theta(k) \approx \theta(k-1) + \frac{T_c}{2} (\omega(k) + \omega(k-1)) \end{cases} \quad (8)$$

and the expression of the distance of the sonar from the wall

$$z(k) \approx |(x(k) + D_x - x_m) \sin \gamma - (y(k) + D_y - y_m) \cos \gamma|. \quad (9)$$

The quantities D_x and D_y are the components expressed in the Cartesian space of the line segment joining the sonar and the robot's centerpoint, i.e. (see Fig. 1)

$$\begin{cases} D_x = \Delta_y \sin \theta - \Delta_x \cos \theta \\ D_y = -\Delta_y \cos \theta - \Delta_x \sin \theta \end{cases}$$

3 Global Solution to RWFP and Sensor Fusion

In this section we propose a solution to RWFP that satisfies the constraints (6)-(7) and provides better estimates, thus overcoming the difficulties mentioned above. We first consider the orientation constraint (6). Then, a time-scaling algorithm will be proposed in order to fulfill the velocity constraint (7). Finally, an EKF merging the information provided by the incremental encoders with the data coming from the sonar will be employed for the estimation of the coordinates (x, y, θ) of the robot.

3.1 Controller with Orientation Constraints

As mentioned above, sonars return significant measurements if their orientation w.r.t. the wall satisfies the orientation constraint (6). We modify the control law (4) as follows:

$$\begin{cases} v = v_{des} \\ \omega = -\frac{k(d-d^0)}{v_{des}} - (\beta_0 + \beta_1 |d-d^0|) \tan(\theta - \gamma) \end{cases} \quad (10)$$

where β_0, β_1 are scalar gains.

Theorem 1 Consider the closed-loop system (1),(10), and let $\beta_0 \geq 0$,

$$\beta_1 \triangleq \frac{k}{v_{des} \tan \sigma_{max}}.$$

Then, for every initial condition $(x(0), y(0), \theta(0))$ with $|\theta(0) - \gamma| \leq \sigma_{max}$, the RWFP is solved, in that

$$|\theta(t) - \gamma| \leq \sigma_{max}, \quad (11)$$

for all $t \geq 0$, and

$$\begin{cases} d(t) \rightarrow d^0; \\ \dot{d}(t) \rightarrow 0; \\ \theta(t) \rightarrow \gamma. \end{cases} \quad (12)$$

as $t \rightarrow \infty$.

Proof: By setting $x_1 \triangleq d - d^0$, $x_2 \triangleq \dot{d}$, the closed-loop equations (1),(10) have the form

$$\begin{cases} \dot{x}_1 = x_2 \\ \dot{x}_2 = -k x_1 \cos \theta - x_2 (\beta_0 + \beta_1 |x_1|) \end{cases} \quad (13)$$

The orientation constraint (11) induces the feasible set

$$S \triangleq \left\{ \begin{bmatrix} x_1 \\ x_2 \end{bmatrix} : |x_2| \leq v_{des} \sin \sigma_{max} \right\}$$

By the particular value of β_1 , it follows that $\dot{x}_2 \leq 0$ for $x_2 = v_{des} \sin \sigma_{max}$, and $\dot{x}_2 \geq 0$ for $x_2 = -v_{des} \sin \sigma_{max}$. Thus, fulfillment of (11) for all $t \geq 0$ is guaranteed for all the initial conditions satisfying (11) at time $t = 0$. We wish to prove stability by applying LaSalle's Theorem [17]. For this purpose, let $\sigma_{max} < 90^\circ$ and consider the following function

$$V(x_1, x_2) \triangleq kx_1^2 + \frac{x_2^2}{\sqrt{1 - \frac{x_2^2}{v_{des}^2}}}$$

and its derivative along the trajectories of the system

$$\dot{V}(x_1, x_2) = -\frac{2x_2^2 (\beta_0 + \beta_1 |x_1|)}{\sqrt{1 - \frac{x_2^2}{v_{des}^2}}} \left[1 + p(x_1, x_2) + \frac{x_2^2}{2v_{des} \left(1 - \frac{x_2^2}{v_{des}^2}\right)} \right] \quad (14)$$

where

$$p(x_1, x_2) = \frac{k}{2v_{des}^2 (\beta_0 + \beta_1 |x_1|)} \frac{x_1 x_2}{\sqrt{1 - \frac{x_2^2}{v_{des}^2}}}$$

For all $(x_1, x_2) \in S$, it holds

$$(\beta_0 + \beta_1 |x_1|)p(x_1, x_2) \geq \beta_0 + k|x_1| \frac{2 - 3 \sin^2 \sigma_{max}}{2v_{des} \sin \sigma_{max} \cos \sigma_{max}}$$

and hence $p(x_1, x_2) > 0$ for $\sigma_{max} \leq 54^\circ$. Since this condition is satisfied by the adopted ultrasonic devices, $\dot{V} \leq 0$ for all $(x_1, x_2) \in S$. Since V is proper in S , and therefore the trajectories of the system are bounded, LaSalle's Theorem guarantees that the origin is globally asymptotically stable in S if the origin is the unique

invariant such that $\dot{V} = 0$. To prove this, let us first suppose that $\beta_0 > 0$. In this case, $\dot{V} = 0$ iff $x_2 = 0$. Since on the x_1 -axis $\dot{x}_2 = -kx_1 \cos \theta$, only the origin is invariant. If $\beta_0 = 0$, then $\dot{V} = 0$ even when $x_1 = 0$. Also in this case it easily follows that the origin is the unique invariant. \square

Remark 1 Theorem 1 does not provide a specific value for β_0 . Indeed, simulations show that, for small values of β_0 , the magnitude of the angular velocity is small enough to avoid sudden rotations of the robot during both steady state and transient operations. The latter fact can be explained by the balance between the contribution due to the position error ($d - d^0$) and the one due to the orientation error ($\theta - \gamma$). However, simulations also show that larger values of β_0 guarantee better robustness against noise and model uncertainty. Thus, the parameter β_0 should be experimentally tuned for the specific application. In our case, we have found that β_0 can be fixed in accordance with the formula $\beta_0 = \alpha \beta_1$, where $\alpha \in [0.05, 0.1]$.

3.2 Velocity Constraints

The control law (10) does not take into account the physical constraints on the wheel velocities, that are summarized in (7). These constraints can be satisfied by on-line scaling the output of the controller as follows. Set

$$\omega = \gamma \omega_\gamma \quad (15)$$

$$v = \gamma v_{des} \quad (16)$$

where ω_γ is given by the r.h.s. of (10) and $v_{des} < r\Omega_{max}$ is the desired linear velocity. The idea is to select on-line γ , $0 \leq \gamma \leq 1$, in order to fulfill the prescribed constraints (7). It is easy to show that by setting

$$\gamma \triangleq \max \left\{ 1, \left| \frac{v_{des} \pm e\omega_\gamma}{r\Omega_{max}} \right| \right\}^{-1} \quad (17)$$

these are in fact satisfied. In order to investigate how the introduction of (17) affects the asymptotical properties of the control scheme, let

$$\tau \triangleq \int_0^t \gamma(\sigma) d\sigma.$$

Then,

$$\begin{cases} \frac{\partial y}{\partial \tau} = v_\gamma \sin \theta \\ \frac{\partial \theta}{\partial \tau} = \omega_\gamma \end{cases}$$

and hence (15)-(16) can be interpreted as a time-varying time-scaling. Then, the same proof of Theorem 1 can be repeated by expressing the dynamics of the system in the new time-reference τ . In particular,

$$\lim_{\tau \rightarrow \infty} \omega(\tau) = 0$$

Then, being $v_{des} < r\Omega_{max}$, there exists τ_f such that $\gamma(\tau) = 1$, $\forall \tau \geq \tau_f$, $\forall t \geq T_f \triangleq \int_0^{\tau_f} \gamma^{-1}(\sigma) d\sigma$. Notice that for $t \geq T_f$, system (1) is driven by the unscaled controller (10), and hence the original asymptotical convergence properties proved in Theorem 1 remain unchanged.

3.3 Extended Kalman Filter (EKF)

Here, we propose an EKF for estimating the coordinates (x, y, θ) of the robot. Let us introduce the vectors

$$\begin{aligned} X(k) &\triangleq [x(k), y(k), \theta(k)]' \\ V(k) &\triangleq [v(k), \omega(k)]' \end{aligned}$$

and denote by $r(X(k))$ the distance of the sonar from the wall, i.e.,

$$r(X(k)) \triangleq |(x(k) + D_x - x_m) \sin \gamma - (y(k) + D_y - y_m) \cos \gamma|.$$

Furthermore, let $E_x(k)$ be a random vector (with zero-mean and covariance matrix $Q_x(k)$) which takes into account noise and model uncertainties, and $\xi(k)$ a random variable (with zero-mean and covariance σ_r^2) modeling the noise affecting the sonar measurement.

For the resulting nonlinear model

$$\begin{cases} X(k) = F(X(k-1), V(k)) + E_x(k) \\ z(k) = r(X(k)) + \xi(k), \end{cases} \quad (18)$$

the equations of the EKF have the form

$$\begin{aligned} P_x(k|k-1) &= J_x(k-1)P_x(k-1|k-1)J_x'(k-1) + \\ &+ J_v(k)P_{v_r}(k|k) + Q_x(k) \\ G_x(k) &= \frac{P_x(k|k-1)H'(k)}{H(k)P_x(k|k-1)H'(k) + \sigma_r^2} \\ P_x(k|k) &= [I - G_x(k)H(k)]P_x(k|k-1) \\ \hat{X}(k|k-1) &= F(\hat{X}(k-1|k-1), \hat{V}(k|k)) \\ \hat{X}(k|k) &= \hat{X}(k|k-1) + G_x(k)[z(k) - r(\hat{X}(k|k-1))] \end{aligned}$$

where $P_{v_r}(i|j)$ is the estimate of the covariance matrix of $V(k)$ at time i based on the information available at time j , $P_x(i|j)$ the estimate of the covariance matrix of $X(k)$, $\hat{X}(i|j)$ the estimate of vector X , $G_x(k)$ the Kalman gain, and $J_V(k)$, $J_X(k)$, and $H(k)$ the Jacobian matrices of (8),

$$\begin{aligned} J_X(k-1) &= \frac{\partial F(X,V)}{\partial X} \Big|_{X=X(k-1), V=V(k)} \\ J_V(k) &= \frac{\partial F(X,V)}{\partial V} \Big|_{X=X(k-1), V=V(k)} \\ H(k) &= \frac{\partial r(\hat{X}(k))}{\partial X} \end{aligned}$$

The filter is initialized by letting

$$\begin{aligned} P_x(0|0) &= \text{Var}[X(0)] \\ \hat{X}(0|0) &= E[X(0)] \end{aligned}$$

where $\text{Var}[X(0)]$ takes into account the degree of precision of the estimate $E[X(0)]$ of the starting coordinates of the robot. The performance of the EKF, is depicted in Fig. 2.

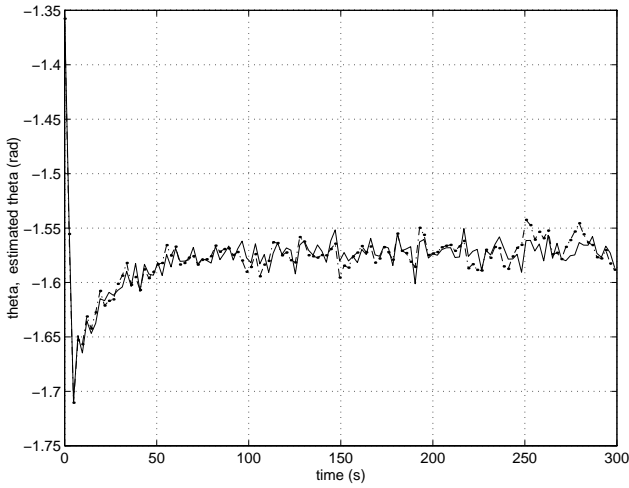


Figure 2: Estimate (—) provided by the EKF and real (---) orientation of the robot

3.4 Control law with EKF

Ultrasonic and velocity measurements are plugged into the control law (10), (17) as follows:

$$\begin{cases} v = \gamma v_{des} \\ \omega = -\gamma \left[\frac{k(z + \Delta_y - d^0)}{v_{des}} + (\beta_0 + \beta_1 |z + \Delta_y - d^0|) \tan(\hat{\theta} - \gamma) \right] \end{cases} \quad (19)$$

where z represents the distance measured with the ultrasonic sensor, and $\hat{\theta}$ is provided by the EKF. Notice that, despite the estimates \hat{x} , \hat{y} are not used in (19), they are typically required by the higher level task for which the proposed wall-following controller is adopted.

4 Experimental Results

The performance of the wall-following controller developed in the previous sections has been tested on the mobile system U.L.I.S.S.E. (Unicycle-Like Indoor Sonar Sensing Explorer) [18, 19] built in the Dipartimento di Sistemi e Informatica of the University of Florence, Italy. It is a cylindrical robot with two driving wheels ($r = 0.056$ m, $e = 0.189$ m). The hardware architecture is based on the 68HC11F1FN Motorola microcontroller [20]. The robot is equipped with 5 sonar sensors (PID604142 Polaroid, [21]) evenly placed around a 180° angle. Only one of the sonars has been used in the current application.

For the wall following defined by $x_m = y_m = 0$, $\gamma = -90^\circ$ and $d^0 = 0.5$ m, the trajectories obtained by using the control law (19) and the EKF developed in Section 3.3 are reported in Fig. 3. The control parameters are: $k = 0.25$ s $^{-2}$, $\beta_0 = 1.3$ s $^{-1}$, $\beta_1 = 26$ m $^{-1}$ s $^{-1}$, $v_{des} = 0.08$ ms $^{-1}$.

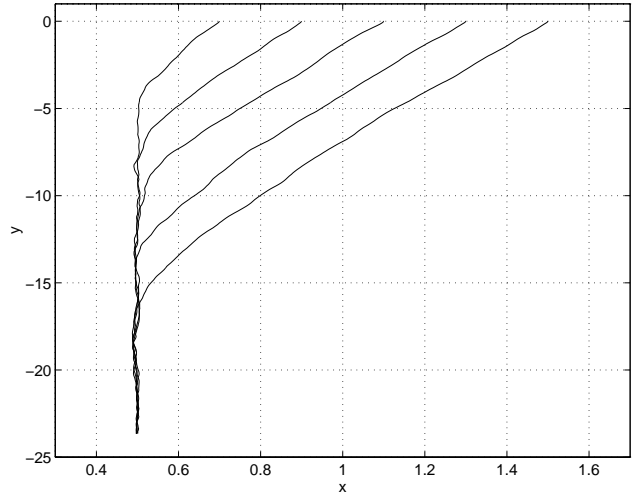
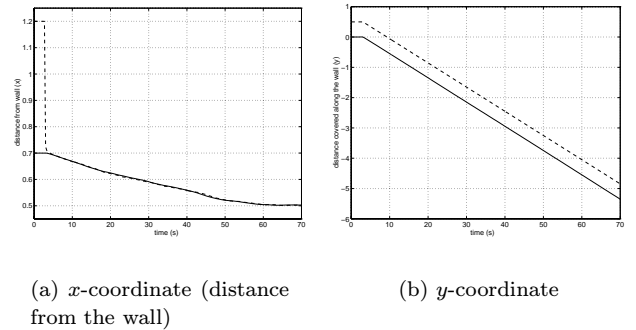


Figure 3: Wall following from different starting positions, control law (19)+EKF.



(a) x -coordinate (distance from the wall)

(b) y -coordinate

Figure 4: Evolution of the coordinates: real (solid line) and estimated (dashed-line)

4.1 Robustness vs. Initial Condition Errors

We investigated the robustness of the control law (19) w.r.t. errors on the starting position and orientation of the robot. In fact, these are often known roughly, in particular when obtained as estimates after a previous run. Figures 4, and 5 show the evolutions of the actual coordinates (solid line) and the corresponding estimates (dashed line) provided by the EKF during a wall following ($x_m = y_m = 0$, $\gamma = -90^\circ$, $d^0 = 0.5$ m), when the $x(0)$ and $y(0)$ are not known. Notice that the initial error on the y -coordinate does not decrease appreciably. In fact, the EKF is updated by the error between the predicted and the measured distance of the robot from the wall. Moreover, the sensitivity w.r.t. orientation and position errors is different: the former directly affects the control action (19), the latter only acts through $\hat{\theta}$, and hence its effect is damped by the EKF. Experimental results show that errors on the starting orientation up to $10^\circ - 15^\circ$ (half of the sonar beamwidth) can be tolerated, while larger errors caused a “loss of contact” with the wall. However,

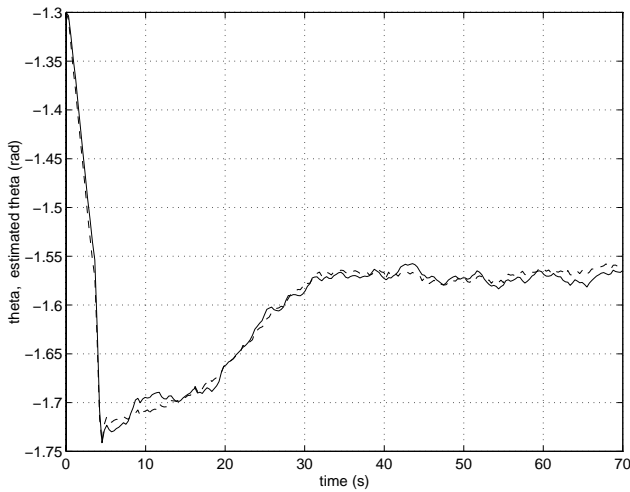


Figure 5: Evolution of the θ -coordinate: real (solid line) and estimated (dashed-line).

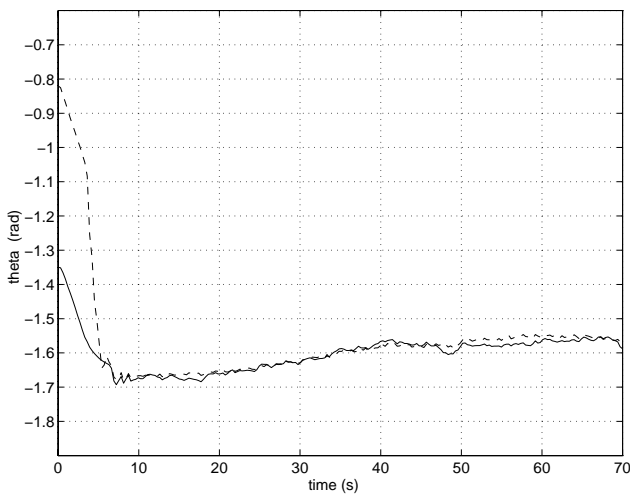


Figure 6: Evolution of the θ -coordinate: real (solid line) and estimated (dashed-line).

higher level strategies have been adopted [22] to reduce the effect of the error on the starting conditions. Such strategies consist in running the EKF while the robot moves under open-loop commands, and switching the wall-following control law on as the orientation error has decreased to acceptable values. As an example, Fig. 6 reports the correction of an orientation error of approximately 30° .

5 Conclusions

For the wall following problem we have presented a control scheme for mobile robots which guarantees orientation and velocity constraint fulfillment, global convergence properties, and also gives an estimate of the robot's position by merging both odometry and ultrasonic measurements. We believe that the proposed solution will serve as a component of more complex ar-

chitectures for map-building and indoor navigation.

References

- [1] P. van Turenout, G. Honderd, and L.J. van Schelven. Wall-following control of a mobile robot. In *Proceedings of the 1992 IEEE International Conference on Robotics and Automation*, pages 280–285, May 1992.
- [2] A. Zelinsky. Mobile robot map making using sonar. *Journal of Robotics System*, 8(5):557–577, 1991.
- [3] J.L. Crowley. Navigation for an intelligent mobile robot. *IEEE Journ. Rob. Automat.*, RA-1(1):31–41, 1985.
- [4] J.C. Latombe. *Robot Motion Planning*. KAP, Boston, 1991.
- [5] J. Borenstein and L. Feng. Measurement and correction of systematic odometry errors in mobile robots. *IEEE Trans. Robot. Automat.*, 12(6):869–880, 1996.
- [6] I.J. Cox. Blanche—an experiment in guidance and navigation of an autonomous robot vehicle. *IEEE Trans. Robot. Automat.*, 7(2):193–204, 1991.
- [7] F. Benayad-Cherif, J. Maddox, and L. Muller. Mobile robot navigation sensors. *SPIE Mobile Robots*, 1831:378–387, 1992.
- [8] J.J. Leonard and H.F. Durrant-Whyte. Mobile-robot localization by tracking geometric beacons. *IEEE Transactions on Robotics and Automation*, 7(3):376–382, 1991.
- [9] H. Durrant-Whyte. Where am I? *Industrial Robot*, 21(2):11–16, 1992.
- [10] A.A. Holenstein and E. Badreddin. Mobile-robot positioning update using ultrasonic range measurements. *International Journal of Robotics and Automation*, 9(2):72–80, 1994.
- [11] J. Borenstein and Y. Koren. Histogramic in-motion mapping for mobile robot obstacle avoidance. *IEEE Trans. Robot. Automat.*, 7(4):535–539, 1991.
- [12] Ö. Bozma and R. Kuc. Building a sonar map in a specular environment using a single mobile sensor. *IEEE Transaction on Pattern Analysis and Machine Intelligence*, 13(12):1260–1269, 1991.
- [13] A. Elfes. Sonar-based real-world mapping and navigation. *IEEE Journal of Robotics and Automation*, RA-3(3):249–265, 1987.
- [14] H. Peremans, K. Audenaert, and M. van Campenhout. A high-resolution sensor based on tri-aural perception. *IEEE Transactions on Robotics and Automation*, 9(1):36–48, 1993.
- [15] P.J. McKerrow. Echolocation - from range to outline segments. *Robotics and Autonomous Systems*, 11:205–211, 1993.
- [16] R. Kuc. A spatial sampling criterion for sonar obstacle detection. *IEEE Transaction on Pattern Analysis and Machine Intelligence*, 12(7):686–690, 1990.
- [17] H.K. Khalil. *Nonlinear Systems*. Macmillan Publishing Company, New York, 1992.
- [18] G. Perugini. Progetto e realizzazione di un robot mobile per la navigazione automatica basata su sensori ad ultrasuoni. Tesi di Laurea, Università degli Studi di Firenze, Facoltà di Ingegneria, 1995.
- [19] L. Tommasi. Analisi e valutazione delle prestazioni di sistemi sonar per applicazioni di robotica mobile. Tesi di Laurea, Università degli Studi di Firenze, Facoltà di Ingegneria, 1996.
- [20] Motorola. *MC68HC11F1 Reference Manual*.
- [21] Polaroid Corporation, Cambridge, Mass. *Ultrasonic Range Finders*, 1982.
- [22] M. Di Marco. Realizzazione di un simulatore di robot mobili per applicazioni di navigazione automatica. Tesi di Laurea, Università degli Studi di Firenze, Facoltà di Ingegneria, 1997.